



UvA-DARE (Digital Academic Repository)

The absence of Ser389 phosphorylation in p53 affects the basal gene expression level of many p53-dependent genes and alters the biphasic response to UV exposure in mouse embryonic fibroblasts

Bruning, O.; Bruins, W.; Jonker, M.J.; Zwart, E.; van der Hoeven, T.V.; Pennings, J.L.A.; Rauwerda, H.; de Vries, A.; Breit, T.M.

DOI

[10.1128/MCB.01610-07](https://doi.org/10.1128/MCB.01610-07)

Publication date

2008

Published in

Molecular and Cellular Biology

[Link to publication](#)

Citation for published version (APA):

Bruning, O., Bruins, W., Jonker, M. J., Zwart, E., van der Hoeven, T. V., Pennings, J. L. A., Rauwerda, H., de Vries, A., & Breit, T. M. (2008). The absence of Ser389 phosphorylation in p53 affects the basal gene expression level of many p53-dependent genes and alters the biphasic response to UV exposure in mouse embryonic fibroblasts. *Molecular and Cellular Biology*, 28(6), 1974-1987. <https://doi.org/10.1128/MCB.01610-07>

General rights

It is not permitted to download or to forward/distribute the text or part of it without the consent of the author(s) and/or copyright holder(s), other than for strictly personal, individual use, unless the work is under an open content license (like Creative Commons).

Disclaimer/Complaints regulations

If you believe that digital publication of certain material infringes any of your rights or (privacy) interests, please let the Library know, stating your reasons. In case of a legitimate complaint, the Library will make the material inaccessible and/or remove it from the website. Please Ask the Library: <https://uba.uva.nl/en/contact>, or a letter to: Library of the University of Amsterdam, Secretariat, Singel 425, 1012 WP Amsterdam, The Netherlands. You will be contacted as soon as possible.

Chapter 3

Absence of Ser389 phosphorylation in p53 affects the basal gene-expression level of many p53-dependent genes and alters the biphasic response to UV exposure in MEFs

Submitted for publication

Wendy Bruins
Oskar Bruning
Martijs J. Jonker
Edwin Zwart
Tessa V. van der Hoeven
Jeroen L.A. Pennings
Harry van Steeg
Timo M. Breit
Annemieke de Vries

Abstract

Phosphorylation is an important post-translational modification event activating the p53 protein to fulfill its role in several cellular processes like apoptosis and cell-cycle arrest. More specifically, with the use of p53.S389A mutant mice and cells, phosphorylation of p53.S389 has been shown, to be at least partly required for several p53 functions, such as the suppression of DNA damage induced skin- and bladder cancer and the induction of apoptosis after UV exposure in mouse embryonic fibroblasts (MEFs). In this study microarray technology for gene-expression analysis was used to identify the molecular and cellular processes underlying this UV phenotype in p53.S389A MEFs.

Intriguingly, absence of p53.S389 phosphorylation already resulted in differential expression of many genes in primary cultured p53.S389A cells compared to wild-type MEFs. For almost all genes these basal expression levels are intermediate between those of wild-type and p53^{-/-} MEFs. Looking at overrepresentation of GO-terms, several cancer-related processes could be attributed to these genes, like the Wnt-pathway, that apparently require p53.S389 phosphorylation to be properly regulated.

In response to UV exposure, we identified a strictly biphasic response in wild-type MEFs, showing an early response three hours after UV exposure and a late response from 12 to 24 hours. Each response phase involved a distinct set of genes. The early stress response results in the direct activation of processes to prevent accumulation of sustained DNA damages in cells, whereas the late response seems more related to re-entering the cell cycle. In our p53.S389A mutant MEFs we identified loss, as well as gain of a number of DNA damage response related processes after exposure to UV, like cell cycle regulation, apoptosis and DNA repair. Furthermore, a large group of genes involved in p53-dependent responses to DNA damage like apoptosis and cell cycle arrest showed an aberrant expression level in p53.S389A MEFs. These results show that phosphorylation of p53.S389 seems essential for an optimal p53-related transcriptional response both endogenously as well as after the induction of DNA damage, ultimately to avoid accumulation of DNA damages and fixation into mutations.

Introduction

UV radiation activates cellular stress responses involving induction of the transcription factor p53. P53 is a DNA damage sensor preventing accumulation of genetic lesions and thus tumor development. To achieve this, the protein is active in a variety of cellular processes, for instance; cell cycle arrest, DNA repair, apoptosis, and senescence [reviewed in [1;2]], predominantly through transcriptional activation of its target genes. Upon UV exposure, p53 halts cell proliferation, allowing cells to repair their DNA damage. However, if a particular cell has an extensive, likely non-repairable amount of DNA damage, p53 initiates apoptosis to prevent the damaged cell from dividing [3]. If these p53-dependent protective cellular responses are compromised or completely absent, accumulation of mutations may lead to genomic instability and finally, to the development of cancerous lesions.

In non-stressed cells, p53 protein is kept at low levels through proteasome-mediated degradation, regulated by ubiquitination. Upon exposure to stress signals, the protein becomes stabilized and activated through post-translational modifications [4]. These p53 protein modifications are quite diverse, as p53 can be phosphorylated, acetylated, ubiquitinated, sumoylated, glycosylated, methylated, and neddylated. The most frequently occurring p53 post-translational modification is phosphorylation.

It is well known that different stressors induce specific p53 modifications [5-8]. Most stressors activate more than one kinase, leading to phosphorylation of p53 at multiple sites. For example, in human cells, DNA damage induced by ionizing radiation or UV irradiation results in (de)phosphorylation of at least 14 different phosphorylation sites; i.e., serine residue 6 (Ser 6), Ser9, Ser15, Ser20, Ser33, Ser37, and Ser46 plus threonine 18 (Thr18) and Thr81 in the amino-terminal region; Ser315 and Ser392 in the C-terminal domain; and Thr150, Thr155 and Ser149 in the central core. Interestingly, the most commonly used stressors, UV irradiation and gamma irradiation, lead to partly different modifications of p53. To illustrate; phosphorylation of human Ser392 (equivalent to mouse Ser389) is specifically triggered after UV irradiation, but not after gamma irradiation [9;10].

The role and significance of p53 phosphorylation has initially been investigated using various *in vitro* model systems. Although these experiments revealed important insights, results were highly contradictory. Later, mouse models with targeted germ line mutations were used to identify the significance of the specific phosphorylation events *in vivo* [recently reviewed in [11]]. Taken together, these studies showed that alterations of amino acids that are involved in the post-translational modifications have a minor impact on p53 functioning compared to p53 mutations identified in human tumors. However, these sites are definitely needed for fine-tuning the p53 stress response, since most of them showed an affected apoptotic or cell-cycle arrest response after exposure to DNA damage.

To investigate the significance of the Ser389 phosphorylation site, we generated mice with a single point mutation in the p53 gene that resulted in a substitution of a serine to an alanine; the p53.S389A mouse model [12]. Cells isolated from p53.S389A mutant mice were partly compromised in their UV radiation induced p53 regulated apoptosis, whereas gamma irradiation induced responses were not affected [12]. In addition, this mutant mouse model displayed increased sensitivity to UV-induced skin- and 2-AAF induced urinary bladder tumor development. This clearly demonstrates the importance of Ser389 phosphorylation for the tumor suppressive function of p53 [12;13]. The impact of Ser389 phosphorylation on the role of p53 functioning as a transcription factor has not been established yet. For this, we have recently used microarray technology for genome-wide transcriptome analysis of the cellular processes underlying the 2-AAF induced cancer-prone phenotype in urinary bladder tissue *in vivo* [14]. We identified delayed gene activation after exposure to 2-AAF of a number of p53 target genes involved in apoptosis and cell cycle control. So, effects of absence of p53.S389 phosphorylation on gene activation could be detected *in vivo* following this genomics approach.

In this study we used UV as a DNA damaging agent to investigate the role of p53.S389 phosphorylation in stress responses. The UV irradiation induced predominantly DNA damage to cells in the form of pyrimidine dimers and 6-4 photoproducts. These lesions are repaired by the nucleotide excision repair (NER) system [15;16]. The response to UV irradiation is complex and involves several pathways [17]. More specifically, Fos/Jun and some growth factors are activated within a few minutes after exposure [18]. Guo *et al.* analyzed the primary UV-induced stress responses in HeLa cells by cDNA microarray analysis [19]. They identified an 'immediate early' UV-C induced stress response 30 to 60 minutes after exposure, with increased activation of (p53-independent) genes like *Egr-1*, *c-Fos*, and *c-Jun*. Studies with murine embryonic stem (ES) cells exposed to DNA-damaging agents, such as UV radiation, have already demonstrated that p53 levels rapidly increase, accompanied by post-translational events resulting in increased transcriptional activity [20-22]. Some p53-dependent genes have been shown to be regulated

upon UV exposure resulting in apoptosis; i.e., *Mdm2*, *Perp*, *Cyclin G* and *Bax* [23]. It was also suggested that *Ets1* might contribute to the specificity of p53-dependent gene transactivation [23], as it is an essential component of the UV-responsive p53 transcriptional activation complex in ES cells. Recent findings showed that both the *ING1b* and *ING2* genes can promote UV-induced apoptosis in a p53-dependent manner in human melanoma cells [24]. These genes enhance the p53-mediated repair of UV radiation-induced DNA damage. Thus far, however, the role of p53 phosphorylation in the broad transcriptome response to UV exposure in primary cells has not been elucidated yet. Here, genome-wide transcriptome analysis was performed on wild-type, p53.S389A and p53^{-/-} MEFs before and after exposure to UV, using an extensive time course analysis. To unravel the role of p53.S389 phosphorylation in the complex UV response in MEFs, we analyzed (i) the effect of absence of p53.S389 phosphorylation on the basal gene-expression levels of p53-dependent genes, (ii) the transcriptome response of wild-type MEFs to UV radiation over time, and (iii) the effect of absence of p53.S389 phosphorylation on UV responses over time. Analysis of the responses on the transcriptome level of p53.S389A MEFs revealed that this p53.S389 phosphorylation site is involved in both the regulation of basal expression levels of a large group of (p53-dependent) genes without any imposed exposure, as well as the altered expression levels of a large group of (p53-dependent) genes in response to UV exposure.

Materials and Methods

Cell culture

Primary mouse embryonic fibroblasts (MEFs) were isolated from E13.5 day embryos. For each genotype the biological variance was spread through the use of five individual embryos obtained from three individual mothers, all in a C57BL/6 background (>F8 generation back crossed). MEFs were cultured as described before [25] in Dulbecco's modified Eagle medium (DMEM Gibco BRL) supplemented with 10% fetal bovine serum (FCS Biocell), 1% non essential amino acids (Gibco BRL), penicillin (0.6 µg/ml) and streptomycin (1 µg/ml) at 37°C and 5% CO₂. The experiment was performed with early passage MEFs (prior to passage five).

UV-treatment

MEFs (five replicates of wild-type, p53.S389A and p53^{-/-}) were expanded, and plated at 1*10⁶ cells per 10 cm plate (Greiner). 24 hours later (~80% confluence) cells were washed with PBS and exposed to UV-C light (20 J/m²). Control samples were mock treated and immediately collected (0 hours). At several time points after treatment (3, 6, 9, 12 and 24 hours), MEFs were rinsed with PBS and collected in 350 µl RLT buffer (enclosed in the RNeasy Mini kit, see RNA isolation).

RNA isolation and preparation of labeled cDNA

Total RNA was isolated using the Rneasy Mini kit (Qiagen, Valencia, CA, USA), followed by a DNase treatment with RNase-Free DNase Set (Qiagen Valencia, CA, USA). RNA was assessed for quality with the Bioanalyzer 2100 (Agilent Technologies, Palo Alto, CA, USA). Both the RNA integrity number (RIN) and the presence or absence of degradation products were checked.

Microarrays, hybridization and validation

The Mouse oligonucleotide libraries (Cat # MOULIBST & Cat # MOULIB384B) were

obtained from Sigma-Compugen Incorporated. Technical support was supplied by LabOnWeb (http://www.labonweb.com/cgi-bin/chips/full_loader.cgi). The libraries represent in total 21,766 LEADS™ clusters plus 231 controls. The oligonucleotide library was printed with a Lucidea Spotter (Amersham Pharmacia Biosciences, Piscataway, NJ, USA) on commercial UltraGAPS slides (amino-silane-coated slides, Corning 40017) and processed according to the manufacturer's instructions. The slides contained 65-mer oligonucleotides and the batch was checked for the quality of spotting by hybridizing with SpotCheck Cy3 labeled nonamers (Genetix, New Milton Hampshire, UK).

Total RNA samples were hybridized in randomized batches, according to a common reference design without dye swap, with embryonic mouse tissue taken as common reference. From the total RNA samples with RIN-value >7, 1.5 µg was amplified using the Amino Allyl MessageAmp aRNA kit (Ambion, Austin, Texas, USA), and labeled with Cy3 (experimental samples) and Cy5 (common reference) reactive dye according to the manufacturer's instructions. The microarrays were hybridized overnight with 200 µl hybridization mixture, consisting of 50 µl Cy3- and Cy5-labeled aRNA (with 150 pMol Cy3 and 75 pMol Cy5), 100 µl Formamide and 50 µl 4 x RPK0325 MicroArray Hybridization Buffer (Amersham Pharmacia Biosciences, Piscataway, NJ, USA) at 37°C and washed in an Automated Slide Processor (Amersham Pharmacia Biosciences, Piscataway, NJ, USA), and subsequently scanned (Agilent DNA MicroArray Scanner, Agilent Technologies, Palo Alto, CA, USA).

To verify the microarray results, cDNA was generated from RNA using the high-Capacity cDNA archive kit containing random hexamer primers (Applied Biosystems). mRNA presence was measured with Taqman gene-expression assays (Applied Biosystems) on a 7500 Fast Real-Time PCR System with a two-step PCR procedure according to the manufacturer's protocol. *Mdm2*; primer forward; TGTGTGAGCTGAGGGAGATGT, primer reversed: ATGCTCACTTACGCCATCGT, Reporter Fam: CTCGCATCAGGATCTTG, *CcnB2*; Mm00432351_m1, *Caspase 8*; Mm0080224_m1, *Pmaip1 (Noxa)*; Mm00451763_m1.

Data extraction and statistical procedure

Microarray spot intensities were quantified as artifact removed densities, using Array Vision software (version 6.0). Further processing of the data was performed using R (version 2.2.1) and the Bioconductor MAANOVA package (version 0.98.8). All slides were subjected to a set of quality control checks, i.e., visual inspection of the scans, examining the consistency among the replicated samples by principal components analysis (PCA), testing against criteria for signal to noise ratios, testing for consistent performance of the labeling dyes, pen grid plots to check consistent pen performance, and visual inspection of pre- and post-normalized data with box plots and ratio-intensity plots.

The data set concerned a two factorial design, with the factors 'Time' (six levels: t = 0, 3, 6, 9, 12, 24 hours) and 'Genotype' (three levels: wild-type, p53.S389A, p53^{-/-}). The design was completely balanced with five replicates each, so the experiment involved 90 observations per gene.

After log₂ transformation, the data were normalized by a spatial lowess smoothing procedure. The data were analyzed using a two stage mixed ANOVA model. First, array, dye and array-by-dye effects were modeled globally. Subsequently, the residuals from this first model are fed into the gene-specific model to fit treatment, and spot effects on a gene-by-gene basis using a mixed model ANOVA. These residuals can be considered as normalized expression values and used in the graphs to depict gene-expression profiles. All fold changes were calculated from the model

coefficients. For hypothesis testing a permutation based F1 test was used (1500 permutations) which allows relaxing the assumption that the data are normally distributed. The significance of differences between factor level means was tested using contrasts. To account for multiple testing, all p-values from the permutation procedure were adjusted to represent a false discovery rate (FDR) of 5%.

Statistical tests

To answer the three research questions defined in the introduction using the microarray data, three different contrast analyses were performed, using the linear modeling procedure described above.

I) For the first research question a gene specific linear model was fitted on the complete data set, which included coefficients for effects of genotype (fixed), time (fixed) and array (random). The significance of each of the three pair wise differences between the three genotypes was tested using a contrast matrix. This test identified genes whose significant difference between mean expression levels between the wild-type, p53.S389A and p53^{-/-} genotype are similar for all time points, and these time profiles can thus be considered parallel. In this study this difference across time is defined as the 'basal' difference in gene expression between genotypes.

II) For the second research question a gene specific linear model was fitted on the wild-type data set containing six time points only, which included coefficients for effects of time (fixed) and array (random). The genes were tested for a main effect among time points. The genes were also subjected to a test for differential gene expression between subsequent time points using a contrast matrix.

III) For the third research question a gene specific linear model was fitted on the complete data set, which included coefficients for each genotype-time combination (fixed) and array (random). The significance of differences in gene expression between subsequent time points for each genotype was tested separately using a contrast matrix. For each time contrast genes were selected that showed a difference between time points in the wild-type MEFs and/or the p53.S389A mutant MEFs.

These three tests yielded three types of gene lists: I) genes with different basal gene-expression levels between the genotypes, II) genes that changed over time that describe a wild-type response to UV irradiation, and III) genes with time specific differences for both the wild-type and p53.S389A MEFs. The immunoglobulin and T-cell receptor genes were deleted from the eventual gene lists, because the probes representing these composite genes were extremely overrepresented in the oligonucleotides libraries.

Additional data analyses

To compare the basal levels of gene expression in the p53.S389A MEFs with the basal levels in the wild-type and the p53^{-/-} MEFs, the model coefficients from analysis (I) were subjected to:

$$y = \frac{|\alpha_{wt} - \alpha_{SA}| + |\alpha_{KO} - \alpha_{SA}|}{|\alpha_{wt} - \alpha_{KO}|}$$

Where α_{wt} , α_{SA} , α_{KO} are the model coefficients quantifying the wild-type, p53.S389A and p53^{-/-} effects respectively. Basically, if the basal level of gene expression of the p53.S389A mutants is higher than p53^{-/-} and lower than wild-type, or lower than p53^{-/-} and higher than wild-type, $y = 1$

by definition. This equation was used to screen for these ‘intermediate responders’.

To relate the differences in gene expression between the wild-type MEFs and p53.S389A MEFs to differences in functional biological processes, the F1-statistics from test (I) and test (III) were used for gene set enrichment analysis (GSEA) [26]. All pathways (Genmapp (Kegg), Biocarta, Sigma Aldrich) present in the c2 database of the Molecular Signature Database (MsigDb 2.0; <http://www.broad.mit.edu/gsea/msigdb>) were tested for significance using the Gene-Set-Test facility provided by the Limma package (version 2.7.3) in Bioconductor. Pathways with p-values ≤ 0.05 and at least five significantly differentially expressed genes from test (I) or test (III) were reported.

This analysis yielded two types of pathway-lists: 1) pathways that are directly related to the difference in basal gene expression between the wild-type and p53.S389A MEFs, and 2) pathways that are related to differences between time points for either the wild-type MEFs or the p53.S389A MEFs.

Lists of differentially expressed genes extracted from test (I), (II) and (III) were all analyzed for overrepresentation of gene ontology’s (GO) using Onto Express (<http://vortex.cs.wayne.edu/projects.htm>). GO-terms with FDR-corrected p-values ≤ 0.1 and at least five significantly differentially expressed genes from test (I), test (II) or test (III) were reported. The assembly of the gene lists for these analyses were driven by biological considerations and based on the results, and is, therefore, described in the results section.

Results

Wild-type, p53.S389A, and p53^{-/-} MEFs were exposed to 20 J/m² UV-C radiation and harvested at different time points after UV exposure (for experimental design, see upper part Figure 1). We previously showed a reduction of total p53 protein levels and a reduced apoptotic response in p53.S389A MEFs compared to wild-type MEFs when exposing to the same dose of UV [12]. A first impression of the differences in gene expression obtained from a PCA is presented in Figure 1 (lower part). This shows a clear separation of the three genotypes along the principal component 1 axis, explaining 32% of total variance. The control samples (i.e., t0) did not cluster, indicating an endogenous difference in basal gene-expression levels (i.e., without UV exposure). The principal component 2 axis, explaining 18% of total variance, shows a clear separation between all time points. Markedly, the time course (including the control samples) after UV exposure of wild-type and p53.S389A MEFs show the same trend along the principal component 2 axis. The 0 and 3 hour time points representing gene expression in p53^{-/-} MEFs also show the same coordinates at this axis however, the 6, 9, 12, and 24 hour time points appear shifted compared to wild-type and p53.S389A MEFs. All together, the gene-expression response of p53.S389A MEFs lies in between that of wild-type and p53^{-/-} MEFs. Expression levels measured by microarray analysis were highly similar to results obtained with real-time PCR (results not shown).

1) The effect of absence of p53.S389 phosphorylation on basal gene-expression levels

To investigate the effect of p53.S389A in MEFs on basal gene-expression levels, we tested for genotype differences. An overall representation of this effect is presented as a ‘volcano’ plot in Figure 2 (upper part). 2,253 genes are affected by the absence of p53.S389 phosphorylation in MEFs (Supplementary Table I, column R; WT_g vs SA_g). To relate these differential genes to functional relevance, we applied gene set enrichment analysis (GSEA). A total of 17 processes

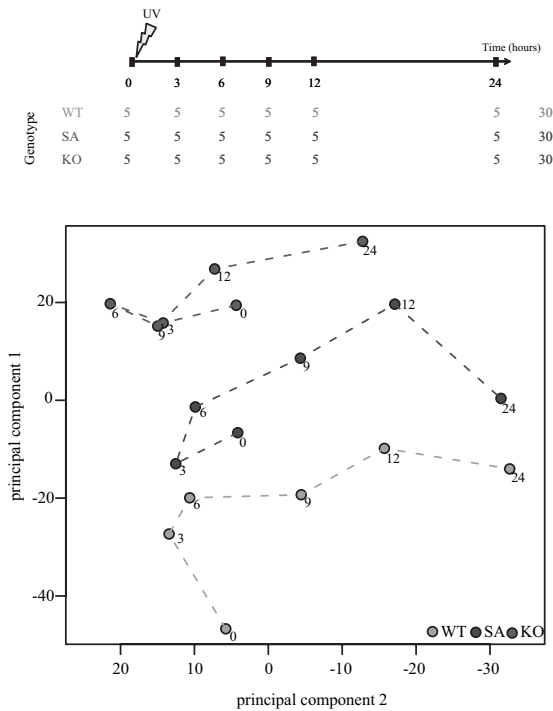


Figure 1 - Experimental design and PCA on microarray data

Upper part: The experimental design depicting the five replicates used at all six time points for the three genotypes; wild-type (WT; green), p53.S389A (SA; blue), and p53^{-/-} (KO; red).

Lower part: Principal Component Analysis (PCA) of all microarray data. The PCA shows segregation between the genotypes on the principal component 1 axis and segregation between the time points on the principal component 2 axis.

For color figure, see page 180.

are significantly affected in p53.S389A MEFs (Figure 2, lower part), comprising one pathway involved in programmed cell death and two pathways related to the Wnt-signaling pathway. The Wnt-signaling pathway is an important pathway involved in a wide panel of developmental and physiological processes like embryogenesis and cancer [27]. Finally, a variety of processes involved in cytoskeleton / chemotaxis and general metabolisms were found to be affected.

Genes affected by the p53.S389A mutation

To classify these 2,253 genes, we identified within these genes 1,762 p53-dependent genes, since these genes are also differentially expressed between wild-type and p53^{-/-} MEFs (again after testing for genotype) (Figure 3A and B). This category of genes needs functional p53 to maintain basal gene-expression levels in MEFs and Ser389 phosphorylation plays a direct role in this. Further classification of 754 genes was achieved by comparison to the genes that were differentially expressed between p53.S389A and p53^{-/-} MEFs. For this category of genes, total absence of p53 or mutated p53.S389A induces a different basal gene-expression level. After grouping, four categories could be identified (Figure 3A and B). The first and by far largest category consisted of 1,128 genes that were affected in their basal gene expression by the mutation at the Ser389 site identical to a complete deletion of p53 (Figure 3A; cat A). The second category consisted of 634 genes that, although affected both by the p53.S389A mutation and p53^{-/-}, the absence of Ser389 phosphorylation had a different effect than a complete deletion of p53 (Figure 3A; cat B). The third category consisted of 120 genes that were unaffected by complete deletion of p53, but phosphorylation of the Ser389 site is nevertheless important to maintain their basal expression level (Figure 3A; cat C). The fourth category consisted of 371 genes that were unaffected by complete deletion of p53, and phosphorylation of the Ser389

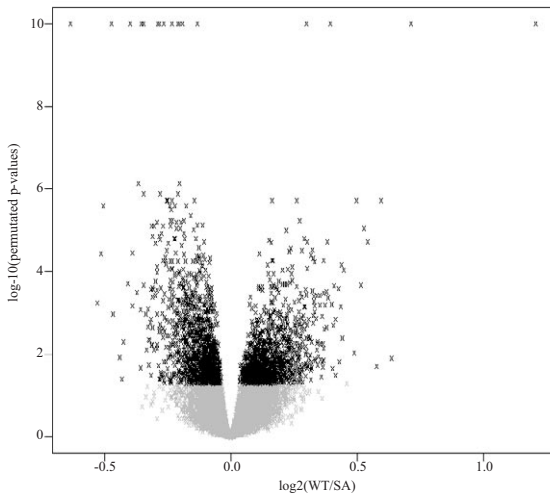


Figure 2 - Volcano plot of basal gene-expression levels in wild-type and p53.S389A MEFs

Upper part: Differences in basal (= without exposure to UV) gene-expression levels between wild-type (WT) and p53.S389A (SA) MEFs. The x-axis shows the relative fold change between wild-type and p53.S389A transformed by log2. When no difference is detected between the gene-expression levels of the two genotypes, the WT/SA ratio =0. The y-axis shows the significance of this difference by indicating the false discovery rate corrected p-values, transformed by $-\log_{10}$. Black dots represent genes with a significantly differentially expressed gene expression changed at the 5% significance level between wild-type and p53.S389A MEFs.

Lower part: Representation of significantly found pathways by gene set enrichment analysis of genes with a significant different basal gene-expression level between wild-type (WT) and p53.S389A (SA) MEFs.

WTvsSA significantly found pathways

ST_GA13_PATHWAY
 ST_DICTYOSTELIUM_DISCOIDEUM_CAMP_CHEMOTAXIS_PATHWAY
 INTEGRIN_MEDIATED_CELL_ADHESION_KEGG
 GLYCEROPHOSPHOLIPID_METABOLISM
 PROSTAGLANDIN_AND_LEUKOTRIENE_METABOLISM
 ST_WNT_BETA_CATENIN_PATHWAY
 SIG_CHEMOTAXIS
 ST_GAQ_PATHWAY
 ST_INTEGRIN_SIGNALING_PATHWAY
 WNT_SIGNALING
 PHENYLALANINE_METABOLISM
 TYROSINE_METABOLISM
 HISTIDINE_METABOLISM
 PROSTAGLANDIN_SYNTHESIS_REGULATION
 SA_PROGRAMMED_CELL_DEATH
 BREAST_CANCER_ESTROGEN_SIGNALING
 KERATINOCYTEPATHWAY

site was only of influence in comparison with the wild-type MEFs (Figure 3A; cat D). (All information: see Supplementary Table I, column V; category WT_g vsSA_g).

Basal expression levels of genes affected by the p53.S389A mutation

Despite being informative, gene classification does not reveal the relative gene-expression levels of the involved genes. Because the PCA showed an overall intermediate response of the genes in p53.S389A MEFs compared to those in wild-type and p53^{-/-} MEFs, we analyzed the relative basal gene-expression levels. For this we defined an ‘intermediate’ basal gene-expression level, simplified characterized as wild-type>p53.S389A>p53^{-/-}, or wild-type<p53.S389A<p53^{-/-}.

1,544 of the 2,253 genes (69%) affected by the p53.S389A mutation were found to have such an ‘intermediate’ basal gene-expression level in p53.S389A MEFs (Figure 3B). Looking specifically at the p53-dependent genes (categories A and B), almost all genes showed an intermediate basal gene-expression level (82% and 98%, respectively). The p53-independent genes (categories C and D) have by definition no intermediate expression levels (see Materials and Methods).

We further analyzed these genes with intermediate basal gene-expression levels to potentially relate p53.S389 phosphorylation to induction (wild-type>p53.S389A) or repression (wild-type<p53.S389A) of p53-dependent genes. The 2,253 genes are almost equally distributed in

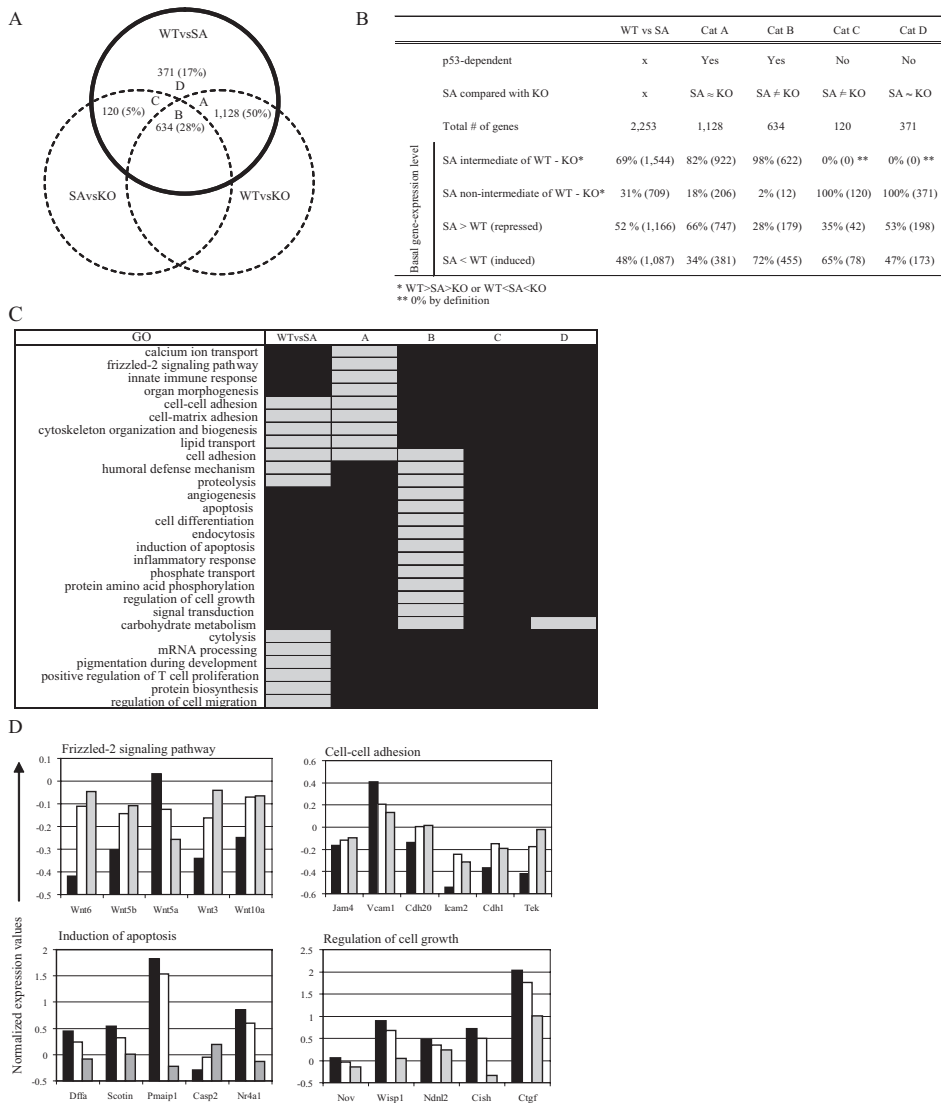


Figure 3 – Differences in basal gene-expression levels between wild-type and p53.S389A MEFs

A) Venn-diagram of genes that showed a differential basal expression level in p53.S389A MEFs compared to wild-type (WTvsSA), classified into four categories by overlap with the genes that gave differential basal expression levels between WT and p53^{-/-} genotype (WTvsKO) and between p53.S389A and p53^{-/-} genotype (SAvsKO). The four indicated categories should be read as:

Category A: P53-dependent genes; absence of Ser389 phosphorylation is similar to p53 loss.

Category B: P53-dependent genes; absence of Ser389 phosphorylation is dissimilar to p53 loss.

Category C: P53-independent genes; absence of Ser389 phosphorylation is dissimilar to p53 loss.

Category D: P53-independent genes; absence of Ser389 phosphorylation is similar to p53 loss.

B) Percentages of genes, in these categories, with - an intermediate basal gene-expression level in p53.S389A compared to wild-type and p53^{-/-} MEFs, or - an assigned p53-repressed/induced trait.

C) The biological significance of genes with a different basal gene-expression level between wild-type and p53.S389A, divided into four categories (for details see text), is identified for overrepresentation of gene ontology's (GO) using Onto Express (p-values ≤ 0.1 and at least five significantly differentially expressed genes).

D) Bar plot of normalized expression values from genes, with a significantly different basal gene-expression level, present in some example processes shown in 3C. Black bars; wild-type, white bars; p53.S389A and grey bars; p53^{-/-}.

p53.S389 phosphorylation-dependent repressed (52%), or induced (48%) genes (Figure 3B). However, 66% of genes in category A are p53.S389 phosphorylation-dependent repressed genes, whereas 72% of category B genes are p53.S389 phosphorylation-dependent induced genes. Category C with 65% is quite identical to category B, whereas for category D almost equal percentages of repressed and induced genes were observed.

Processes involving genes with basal gene-expression levels affected by the p53.S389A mutation

To get further insight in which cellular processes the genes with affected basal gene-expression levels are involved, GO-analyses for overrepresentation of GO-terms were performed (Figure 3C) [28]. 13 significant GO-terms were found for total wild-type versus p53.S389A genotype, 9 for category A, 14 for category B, none for category C, and just 1 for category D. Strikingly, analysis using the categories resulted in the loss of 6 but gain of 15 GO-terms, underlining the meaning of the defined categories. It appears that the more general GO-terms are replaced by more specific GO-terms, especially in category B, such as ‘(induction of) apoptosis’ and ‘protein amino acid phosphorylation’. Moreover, there is only one GO-term overlap between category A and category B.

Combining the results it means that specific processes, represented by the GO-terms found with category A genes, are mostly actively repressed via p53.S389 phosphorylation. Two examples are presented (Figure 3D; upper part) for the ‘Frizzled-2 signaling pathway’ and ‘cell-cell adhesion’ in which 100% and 67% of the respective genes showed an intermediate basal gene-expression level in p53.S389A MEFs, as well as 80% and 83% of the respective genes are expressed higher in p53.S389A than wild-type MEFs. Similarly, specific processes, represented by the GO-terms found with category B genes, are mostly actively induced via p53.S389 phosphorylation. Two examples are presented (Figure 3D; lower part) for the ‘induction of apoptosis’ and ‘regulation of cell growth’ in which 100% of the respective genes showed an intermediate basal gene-expression level in p53.S389A MEFs, as well as 80% and 100% of the respective genes are expressed lower in p53.S389A than wild-type MEFs.

II) Gene-expression analysis of the response to UV exposure in wild-type MEFs

To analyze the role of p53.S389 phosphorylation in the UV response, we started with a gene-expression analysis of the UV response over time in wild-type MEFs. An ANOVA analysis was performed and 6,058 significantly, differentially expressed genes were identified (Supplementary Table I, column S; WT₁). In this set of genes, a total of eight different clusters with a common gene-expression profile were found after hierarchical clustering (Figure 4A). Common gene-expression profile could be identified with predominantly early decrease (1, 2, 3, and 8), continuous decrease (5), late decrease (4), early increase (4 and 6), and late increase (1, 2, 3 and 7).

Phase-specific genes involved in the response to UV exposure in wild-type MEFs

The common gene-expression profiles were quite difficult to interpret, but showed predominantly early and late effects. Therefore, we proceeded by analyzing the relative change in each phase of the time line and 2,856 genes were found differentially expressed in at least one of the five time intervals; t0-3, t3-6, t6-9, t9-12, t12-24 (Figure 4B). This revealed that the UV response primarily takes place 3 hours after exposure (phase I) and 12-24 hours after exposure (phase III),

as most differentially-expressed genes are found there; 1,427 and 1,756 respectively (Figure 4B and C). We defined three phases; I (t0-3), II (t3-6, t6-9, or t9-12), and III (t12-24) and four exclusive categories; Early (923), Middle (107), Late (1,257), and Early-Late (387) responsive genes. There is a rather high specificity of responsive genes with respect to the phases; the Early responders compile 65% of the phase I genes, and the Late responders compile 72% of phase III genes (Figure 4C). The Early-Late responders compile almost the rest of the genes in phase I and III. Strikingly, most of the genes found in t0-3 were down-regulated, whereas those found in t12-24 were mostly up-regulated (results not shown). So, there are two important phases (I and III) in the UV response in wild-type MEFs and these both show involvement of primarily specific genes.

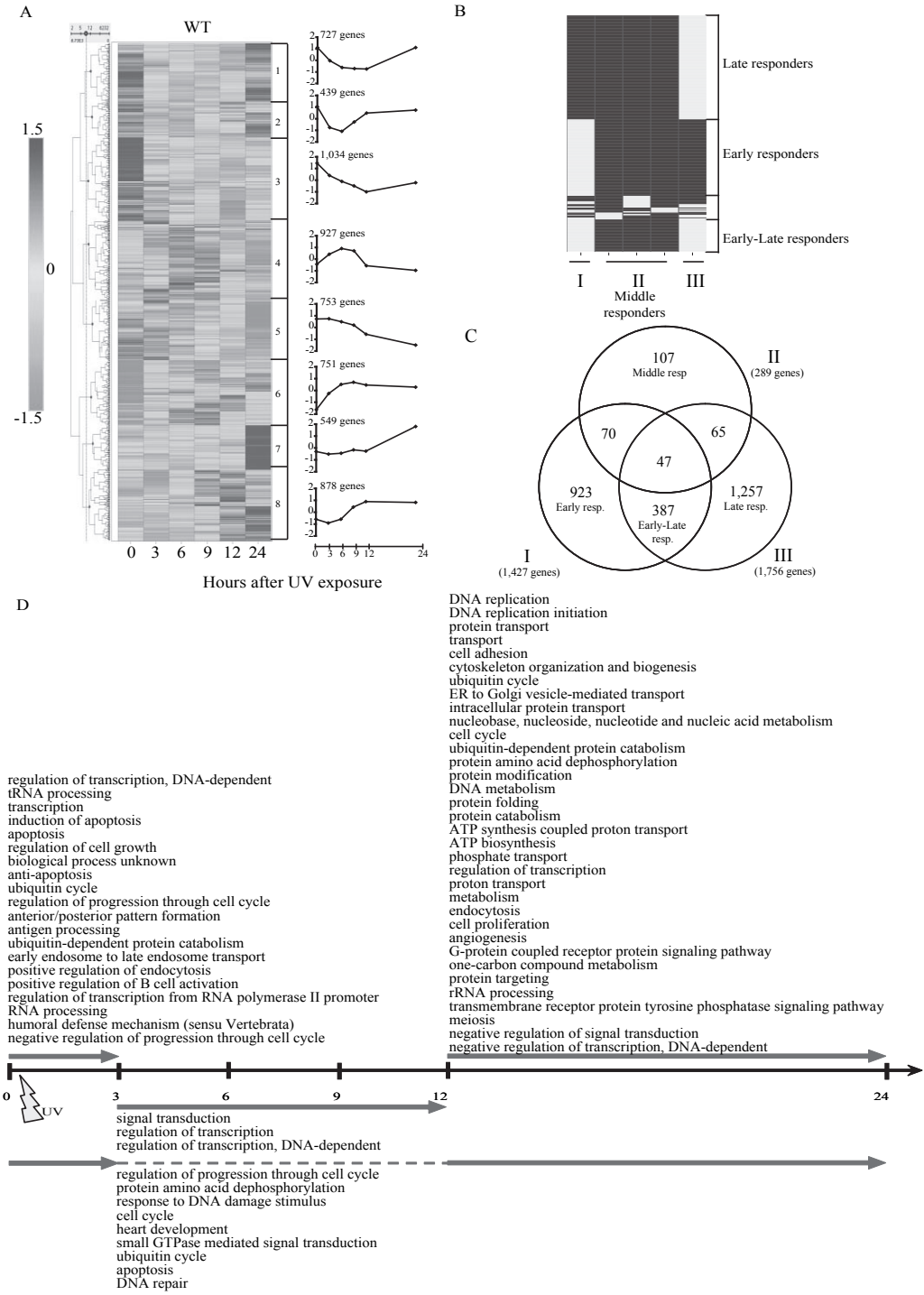
Phase-specific processes involved in the response to UV exposure in wild-type MEFs

To identify the involved cellular processes, we subsequently analyzed the four categories of responsive genes using GO-analysis. As was to be expected from the number of genes involved, we found 20 affected GO-terms with Early, 3 with Middle, 34 with Late, and 9 with Early-Late responsive genes (Figure 4D). There is little overlap between the GO-terms of these four categories.

We did find as expected GO-terms like; 'cell cycle', 'DNA repair', 'regulation of transcription from RNA polymerase II promoter' and '(induction of) apoptosis', as they are implicated before with respect to treatment with a genotoxic agent like UV in a different cellular context [29]. Furthermore, as somewhat expected, processes like 'response to (regulation of) transcription', 'cell adhesion' and 'DNA replication' are significantly present. Also, ubiquitin-related processes like 'ubiquitin cycle' were found significantly affected in response to UV irradiation. Interestingly, looking in more detail at the differences in processes found in the Early, Middle, Late and Early-Late responders, it can be observed that for instance 'regulation of transcription, DNA-dependent' was found significantly affected in the two categories Early and Middle responders, whereas the opposite process 'negative regulation of transcription, DNA-dependent' was found in Late responders. It can finally be concluded that apoptosis-related and cell-cycle regulation processes are involved early after UV exposure, whereas a variety of DNA replication and metabolism processes are involved later in time.

P53 target genes involved in the response to UV exposure in wild-type MEFs

Finally, we determined which of the 6,058 differentially-expressed genes in wild-type MEFs in response to UV were already identified as p53 targets before. For this we used the p53 downstream model of Harris and Levine, comprising important p53 target genes and their function [30]. Figure 6 shows an adapted version of this model as shown before [14] and provides an overview of the genes showing an altered response in our wild-type MEFs in response to UV exposure. The regulator of p53 stability and activity *Mdm2*, as well as *E2f1* were involved in wild-type UV response in MEFs. In almost all depicted downstream pathways, p53 target genes were involved: 70% of the cell cycle arrest pathway, 100% of the extrinsic-apoptotic pathway, 44% of the intrinsic-apoptotic pathway, one (of four) downstream of these apoptotic pathways, and even one (of four tested) in the angiogenesis and metastasis pathway. In summary, profiles of differential gene expression in wild-type MEFs after exposure to UV can be convincingly mapped to specific p53 dependent pathways.



III) Effect of absence of p53.S389 phosphorylation on UV-induced gene expression

After establishing the basic wild-type mechanisms for UV response we continued with a gene-expression analysis of the UV response over time in p53.S389A MEFs. An ANOVA analysis was performed and 4,166 significantly differentially expressed genes were identified (Supplementary Table I, column T;SA_↓), which is substantially lower than the 6,058 genes found in wild-type MEFs. The ANOVA analysis did not show any genes with a significant difference in gene expression over time between wild-type and p53.S389A MEFs after UV exposure (interaction term ‘Genotype’ x ‘Time’). This means that any potential difference in response is likely to be quite subtle, compelling us to use alternative approaches to analyze the gene-expression data.

Genes involved in the UV response of p53.S389A and wild-type MEFs

We integrated all previous analyses at the gene level by mutual comparing the 4,166 p53.S389A UV responsive genes to the 6,058 wild-type UV responsive genes and to the 2,253 genes with a changed basal gene-expression level by the absence of p53.S389 phosphorylation (Figure 5A and Supplementary Table I, column R; WT_g vs SA_g, column S; WT_g; column T; SA_g). 918 genes (41%) with changed basal gene-expression level in p53.S389A MEFs are involved in the response to UV exposure in either wild-type or p53.S389A MEFs. In contrast, 1,335 genes (59%) with a changed basal gene-expression level were not involved in the UV response, but are presumably involved in other cellular processes where p53.S389 phosphorylation plays an important role. Reversely, 2,107 genes (35%) were solely found in wild-type MEFs in response to UV exposure, indicating phosphorylation of p53.S389 is somehow a prerequisite for optimal involvement of these genes in the normal UV response. Also, 544 genes (13%) were solely found in p53.S389A MEFs in response to UV exposure, indicating that absence of phosphorylation of p53.S389 causes involvement of these genes in the p53.S389A UV response. Finally, 3,558 genes were found differentially expressed in both wild-type (59%) and p53.S389A (85%) MEFs in response to UV exposure, which indicates that phosphorylation of p53.S389 is not exclusively needed for the involvement of these genes in the normal UV response.

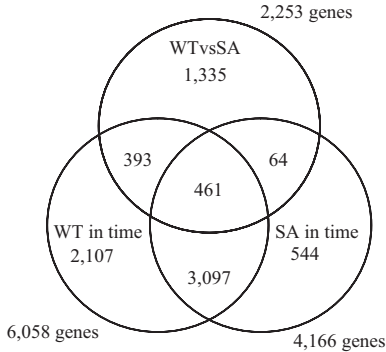
Phase-specific genes involved in the UV response of p53.S389A and wild-type MEFs

From earlier studies [14] we suspected time-related UV responses, such as delayed gene activation, specific to the p53.S389A MEFs. For this, we identified differentially expressed genes in wild-type and p53.S389A MEFs in response to UV applying the previously defined time intervals, i.e., phase I (t0-3), phase II (union of t3-6, t6-9, and t9-12), and phase III (t12-24) (cf. Figure 4B). Combining the results revealed for each phase wild-type specific, wild-type and p53.S389A

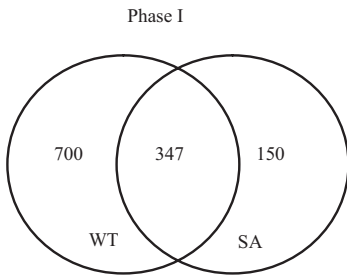
Figure 4 – Affected genes and processes in wild-type MEFs after exposure to UV

- A) Hierarchical clustering of the average log₂ (z-scores) of the 6,058 differentially expressed genes in wild-type (WT) MEFs over time after exposure to UV revealed eight clusters with a common gene-expression profile. Each row represents an individual gene and each column represents a time point after exposure to UV (untreated = 0). The degree of redness and greenness represents induction and repression respectively. (For details, cf. Supplementary Table I)
- B) Clustering of 2,856 differentially expressed genes found by time-period-specific analysis of wild-type MEFs after exposure to UV. Each row represents an individual gene and each column represents a time interval after UV exposure: t0-3, t3-6, t6-9, t9-12 and t12-24. Gene was found (grey) or not-found (black) differentially expressed in a time interval. From this we defined four categories of responsive genes: Early, Middle, Late, and Early-Late.
- C) Venn-diagram illustrating the number of responsive genes found in the defined phases I (t0-3), II (t3-6, t6-9, or t9-12), and III (t12-24).
- D) Significant GO-terms (ranked with decreasing significance) for the four categories of responsive genes, plotted on the phases of the time-line.
- For color figure, see page 181.

A



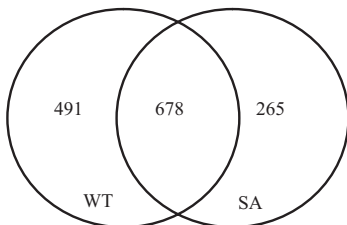
B



Phase II



Phase III



C

Processes in wild-type MEFs not found in p53.S389A MEFs after exposure to UV

| GSEA Pathways | Phase I | Phase II | Phase III |
|--|---------|----------|-----------|
| INTEGRIN_MEDIATED_CELL_ADHESION_KEGG | ■ | | |
| ARAPPATHWAY | ■ | | |
| CELL_CYCLE_KEGG | | | |
| ST_INTEGRIN_SIGNALING_PATHWAY | | | |
| GI_TO_S_CELL_CYCLE_REACTOME | | | |
| ATP_SYNTHESIS | | | |
| FLAGELLAR_ASSEMBLY | | | ■ |
| PHOTOSYNTHESIS | | | |
| APOPTOSIS_KEGG | | | |
| INTEGRINPATHWAY | | | |
| CIRCADIAN_EXERCISE | | | |
| GLYCOSPHINGOLIPID_METABOLISM | | | |
| TYPE_III_SECRETION_SYSTEM | | | |
| Go-categories | | | |
| anterior/posterior pattern formation | ■ | | |
| heart development | ■ | | |
| induction of apoptosis | ■ | | |
| ion transport | ■ | | |
| protein catabolism | ■ | | |
| protein ubiquitination | ■ | | |
| rhythmic process | ■ | | |
| small GTPase mediated signal transduction | ■ | | |
| steroid biosynthesis | ■ | | |
| tRNA processing | ■ | | |
| G-protein coupled receptor protein signaling pathway | | ■ | |
| protein amino acid dephosphorylation | | ■ | |
| regulation of progression through cell cycle | | | ■ |
| cell cycle | | | ■ |
| endocytosis | | | ■ |
| ER to Golgi vesicle-mediated transport | | | ■ |
| meiosis | | | ■ |
| nucleobase, nucleoside, nucleotide and nucleic acid metabolism | | | ■ |
| protein modification | | | ■ |

D

Processes in p53.S389A MEFs not found in wild-type MEFs after exposure to UV

| GSEA Pathways | Phase I | Phase II | Phase III |
|--|---------|----------|-----------|
| HIVNEFPATHWAY | ■ | | |
| SIG_CD40PATHWAYMAP | | | ■ |
| G_PROTEIN_SIGNALING | | | ■ |
| ST_TUMOR_NECROSIS_FACTOR_PATHWAY | | | ■ |
| GLYCEROPHOSPHOLIPID_METABOLISM | | | ■ |
| CALCIUM_REGULATION_IN_CARDIAC_CELLS | | | ■ |
| SMOOTH_MUSCLE_CONTRACTION | | | ■ |
| PURINE_METABOLISM | | | ■ |
| Go-categories | | | |
| cell division | ■ | | |
| intracellular signaling cascade | ■ | | |
| mitosis | ■ | | |
| negative regulation of transcription from RNA polymerase II promoter | ■ | | |
| positive regulation of cell proliferation | ■ | | |
| regulation of apoptosis | ■ | | |
| transport | ■ | | |
| regulation of transcription from RNA polymerase II promoter | ■ | | |
| apoptosis | ■ | | |
| positive regulation of transcription from RNA polymerase II promoter | ■ | | |
| regulation of transcription | ■ | | |
| biosynthesis | ■ | | |
| cell-matrix adhesion | ■ | | |
| lipid transport | ■ | | |
| metabolism | ■ | | |
| neuropeptide signaling pathway | ■ | | |
| protein biosynthesis | ■ | | |
| protein folding | ■ | | |
| proton transport | ■ | | |
| ubiquitin-dependent protein catabolism | ■ | | |

E

Processes found in a different phase in p53.S389A MEFs compared with wild-type MEFs after exposure to UV

| Go-categories | Phase I | Phase II | Phase III |
|---|---------|----------|-----------|
| 1) DNA repair | WT | | SA |
| 2) response to DNA damage stimulus | WT | | SA |
| 3) transforming growth factor beta receptor signaling pathway | WT | | SA |
| 4) protein transport | WT | SA | |
| 5) mRNA processing | | WT | SA |

F

| 1) WT | 1) SA | 2) WT | 2) SA |
|----------------------|----------------------|---------------|---------------|
| 2210018M11Rik | 2210018M11Rik | 2210018M11Rik | 2210018M11Rik |
| Apex2 | Chaf1b | Apex2 | Chaf1b |
| Asf1a | Mre11a | Ercce1 | Mapk1 |
| Ercce1 | Msh2 | Exo1 | Mre11a |
| Exo1 | Nthl1 | Foxo3a | Msh2 |
| Polg2 | Nudt1 | Gadd45a | Nthl1 |
| Polh | Polk | Polh | Polk |
| Rad1 | Smc3 | Rad1 | Smc3 |
| Rad17 | Trex1 | Rad17 | Trex1 |
| Rad18 | Ube2a | Rad18 | Ube2a |
| Smc3 | Ube2b | Smc3 | Ube2b |
| Trex1 | Xrcc1 | Trex1 | Xrcc1 |
| Xab2 | Xrcc4 | Xab2 | Xrcc4 |
| 3) WT | 3) SA | 4) WT | 4) SA |
| Bambi | Bmp8a | Ap2a1 | Atg16l1 |
| Bmpr1a | Bmpr2 | Arfgap1 | Blzf1 |
| Dep1a | Ltbp3 | Atg16l1 | Nup37 |
| Smad2 | Map3k7 | Blzf1 | Rabif |
| Smad7 | Smad7 | Clpx | Rap2b |
| | | Dnajc14 | Rhob |
| | | Dnajc17 | Rras2 |
| 5) WT | 5) SA | | |
| 2600011C06Rik | 5730449L18Rik | Gem | Snx24 |
| 6530403A03Rik | 6530403A03Rik | Kras | Snx7 |
| A1462438 | A1462438 | Necap1 | Tomm40 |
| Gemin7 | Apobec1 | Nup107 | Vps53 |
| Lsm8 | Cdc40 | Nup37 | |
| Sfrs10 | Cstf2 | Nupl2 | |
| Sfrs7 | Cstf3 | ORF28 | |
| Snrpb | Eftud2 | Rab14 | |
| Tsen54 | Fip111 | Rab25 | |
| | Lsm1 | Rab30 | |
| | Lsm8 | Rab5a | |
| | Nudt21 | Rabif | |
| | Prpf40a | Rab14 | |
| | Sf4 | Rnd3 | |
| | Snrpd1 | Rras2 | |
| | | Sefi1 | |
| | | Snag1 | |
| | | Snap23 | |
| | | Snx10 | |
| | | Snx24 | |
| | | Snx7 | |
| | | Tom11 | |
| | | Ube112 | |
| | | Vps33b | |
| | | Xpo1 | |

Figure 5 - Phase-specific genes and processes in wild-type and p53.S389A MEFs after exposure to UV

A) Venn-diagram combining the gene lists of three analysis:

- i) 'WTvsSA', genes with differences in basal expression levels between wild-type (WT) and p53.S389A (SA);
- ii) 'WT in time', genes with over time changing expression in wild-type MEFs after UV exposure;
- iii) 'SA in time', genes with over time changing expression in p53.S389A MEFs after UV exposure.

B) Venn-diagrams per phase of genes involved in wild-type and p53.S389A UV response. For phase definition cf. Figure 4B.

C) Phase and wild-type specific pathways and GO-terms determined on basis of phase and wild-type specific genes.

D) Phase and p53.S389A specific pathways and GO-terms determined on basis of phase and p53.S389A specific genes.

E) GO-terms determined as in C and D, but only genotype specific for a certain phase.

F) Genes involved in showing the wild-type and p53.S389A UV response for GO-terms in 5F. Bold genes are present in both genotypes.

shared, plus p53.S389A specific UV responsive genes (Figure 5B and Supplementary Table II), with the same implication as to the role p53.S389 phosphorylation represents for these genes explained in the previous paragraph. Judging from the fraction (67%) of phase I wild-type specific UV responsive genes as well as the fraction (58%) of the phase III wild-type overlapping p53.S389A UV responsive genes, phosphorylation of p53.S389 seems mostly required in the early phase of normal UV response.

Phase-specific processes involved in the UV response of p53.S389A and wild-type MEFs

To determine the effects of the absence of Ser389 phosphorylation on a process level we performed an integrated GO and GSEA-analysis on these phase specific genes involved in the UV response of p53.S389A and wild-type MEFs. We distinguished phase-specific GO-terms and pathways that were also: genotype-specific for the wild-type UV response (requiring p53.S389 phosphorylation, Figure 5C), genotype-specific for p53.S389A UV response (result of absence of p53.S389 phosphorylation, Figure 5D), and present in both wild-type and p53.S389A UV response but in a different phase (p53.S389A mutation has a different effect in a different phase, Figure 5E). The majority of identified genotype-specific pathways and GO-terms were again in phase I and III. Also, they were extremely specific as there was no genotype-specific pathway or GO-term present in both phases. There were only five phase-specific, genotype non-specific GO-terms, of which three were present in wild-type phase I and p53.S389A phase II (Figure 5E). Although this may hint towards a delayed response, comparison of the individual genes showed that only few genes of these GO-terms were both wild-type as well as p53.S389A specific (Figure 5F).

p53 target genes involved in the UV response and affected by the p53.S389A mutation

Finally, we mapped these results regarding the role of p53.S389 phosphorylation to the previously introduced p53 downstream model of Harris and Levine [30]. Figure 6 shows an overview of the effects of absence of p53.S389 phosphorylation on the wild-type UV response. Of the wild-type UV responsive genes six were not found to be differentially expressed in p53.S389A MEFs, 13 were found to have a lower gene expression in p53.S389A MEFs, and one was found to have a higher gene expression compared to wild-type MEFs. The latter observation of the *Cdc2* gene fits with the reduced expression level of its (indirect) negative regulators, i.e., *Reprimo* and *Gadd45*. More importantly, the apoptotic pathways mainly showed a reduced activity, whereas the cell-cycle arrest pathways seem either off (G1-S) or induced (G2-M) in UV-induced p53.S389A MEFs.

Discussion

Post-translational modifications of p53 are important in regulating p53 stability and activity [7;31]. We showed previously that the p53.S389 phosphorylation site is partial responsible for tumor suppression of UV-induced skin tumors and 2-AAF induced urinary bladder tumors [12-14]. Mutant p53.S389A cells showed an affected apoptosis response after UV exposure [12] and several p53 target genes involved in apoptosis and cell cycle control showed a delayed response in p53.S389A urinary bladders after 2-AAF exposure. Here, we used microarray technology for transcriptome analysis on primary MEFs before and after exposure to UV, to analyze the effect of absence of p53.S389 phosphorylation on apoptosis and other p53-dependent pathways.

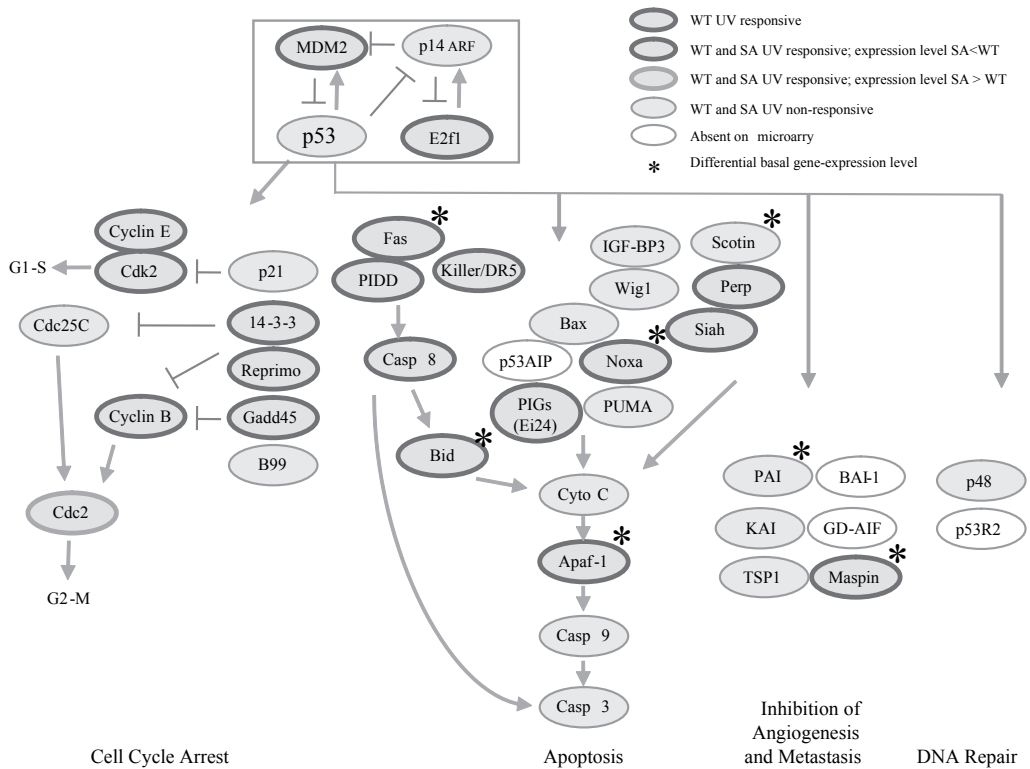


Figure 6 - Affected p53 target genes in wild-type MEFs after exposure to UV

P53 target genes involved in the apoptotic, cell cycle arrest, inhibition of angiogenesis and metastasis, and DNA repair processes are presented in a model adapted from [14;30]. For color figure, see page 182.

1) The effect of absence of p53.S389 phosphorylation on basal gene-expression levels

Phosphorylation of p53.S389 occurs specifically after exposure to DNA damaging agents [32;33], especially UV [9;10], initiating both p53-dependent and p53-independent cellular responses. Given that the level of Ser389 phosphorylated p53 in untreated cells is extremely low [12], cells lacking this specific phosphorylation event supposedly would only be affected in their response to a DNA damaging agent like UV. However, when only considering the genotype (without exposure), we found compared to wild-type: 2,253 genes differentially expressed in p53.S389A MEFs, i.e., p53.S389 phosphorylation dependent genes, as compared to the 7,567 genes differentially expressed in p53^{-/-} MEFs, i.e., p53-dependent genes (results not shown). The overlap was 23% of all p53-dependent genes and 78% of the p53.S389 phosphorylation dependent genes. Although in line with similar observations where the p53.S389A genotype [34] or complete deletion of p53 [34] resulted in altered gene-expression prior to any exposure, the number of genes with adjusted basal gene-expression level seems rather high in the study described here. This phenomenon could be caused by so-called ‘spontaneous’ DNA damages, like reactive oxygen species (ROS) or depurination [reviewed in [35]], since a relation between ROS, p53 protein levels and oxidative damage inducing agents has been described before [36;37]. Another possible explanation could be the *in-vitro* culture conditions, since for instance exposure of cells to 20% O₂ and 6% CO₂ clearly imposes (genotoxic) stress on the cells. However, it is also

plausible to think the whole system might be readjusted as a network to respond to the effect of the introduced p53.S389A mutation. If so, it means that the affected genes are somehow related to normal p53.S389 functioning and their analysis will be extremely informative.

The genes with an altered basal expression level in unexposed p53.S389A are involved in various pathways. Of these, 'cell adhesion' and 'metabolism' were previously also found to be affected by a p53 codon 237 mutation in human lymphoblastoid cells [34]. Furthermore, several *Wnt* genes that are able to activate the important Wnt-signaling pathway, involved in a broad panel of developmental and physiological processes like embryogenesis and cancer [27], showed an increased basal gene-expression level. Since depletion of β -catenin made cells more sensitive to apoptosis [38], the up-regulation of the four *Wnt* genes in p53.S389A mutant MEFs might explain the previously observed reduced apoptotic response [12].

To interpret the p53.S389A phosphorylation dependent genes with adjusted basal expression, we categorized them using basal gene-expression levels in p53^{-/-} MEFs as compared to wild-type and/or p53.S389A MEFs. As such, we were able to identify whether these genes were p53-dependent (SAvsWT = KOvsWT), showed a similar change compared to p53^{-/-} (SA \approx KO), had a basal gene-expression level intermediate to wild-type and p53^{-/-} (WT>SA>KO or WT<SA<KO), and are repressed (WT<SA) or induced (WT>SA) by intact p53.S389 phosphorylation. This turned out to be quite a successful approach. We could identify the p53-independent genes (22%) and from the almost complete lack of results from the GO-analysis, we assumed that these genes, although affected, do not play an important role in the context of p53.S389 phosphorylation. This left us with the p53-dependent genes that almost all (88%) showed a basal gene-expression level in between that of wild-type and p53^{-/-}, meaning that p53.S389 phosphorylation is partly needed for an optimal p53-dependent response of these genes. Moreover, (p53-dependent) genes that are normally p53.S389 phosphorylation-dependently repressed, show mostly (81%) a similar response in the p53.S389A cells and the p53^{-/-} cells, whereas genes that are normally p53.S389 phosphorylation-dependently induced, showed no bias. It might be a general effect that p53-dependent repression of gene-expression can be relieved by just a small p53 modification mutation in a similar fashion as p53 absence would. Likewise, for p53-dependent induction of gene-expression the effect of p53 absence cannot as easily be mimicked, probably due to redundancy in activation mechanisms.

As for the processes related to the defined p53.S389 phosphorylation-dependent gene categories, several GO-terms were found for the p53-dependent genes, such as frizzled-2 signaling pathway, cell adhesion, (induction of) apoptosis, and regulation of cell growth. There appears to be a slight bias for signal transduction and cellular interaction processes to be normally repressed by p53 (Ser389 phosphorylation), whereas other cellular processes seem to be induced by p53.S389 phosphorylation. Specific for cell growth, cultured p53^{-/-} MEFs were shown to grow faster than wild-type MEFs [39], which might also be true for p53.S389A MEFs. However, this assumption is not that obvious, as the process 'regulation of cell growth' was found for p53-induced genes but the gene expression levels in p53.S389A MEFs were closer to wild-type than to p53^{-/-}.

These observations in adjusted basal gene-expression levels might relate to altered responses in p53.S389A MEFs to DNA damaging compounds like UV radiation. One can envision that certain basal levels are preferable when an immediate response to DNA damage (here UV exposure) is required, and cells with certain genotypes lacking these basal levels might have delayed or reduced capacities to initiate the proper response efficiently after DNA damage. This hypothesis is supported by the fact that no less than 41% of the genes with adjusted basal

expression in p53.S389A are also found after UV exposure in either wild-type MEFs (17%), p53.S389A MEFs (3%), or both (20%). Obviously, this leaves 59% (1,335) of the genes that are involved in p53.S389 phosphorylation-dependent processes other than those involved in UV response.

II) Analysis of differentially-expressed genes in wild-type MEFs after UV exposure

Besides several *in vitro* experiments with UV as challenging agent, for instance: rat cardiac myocytes/fibroblasts [40], HeLa cells [19], human skin fibroblasts [41], and human cancer cell lines (MCF-7, H1299, HCT116, Tera1 and IMR32), [42], some studies also included gene-expression analyses, for instance; human melanocytes [43], human keratinocytes, [44;45], cancer cell lines TK6 (p53 wild-type) and NH32 (p53^{-/-}) [46], and keratinocytes (NHEK) [47]. The majority of these studies were carried out with immortalized or cancer cell lines, analyzing gene-expression differences using a limited amount of time points after exposure to UV. These limitations formed our current experiment design to study primary responses to DNA damaging agents at the transcriptional level in primary cells (MEFs) after UV-C exposure with an extensive time course. The consequence, of course, is quite a complex bioinformatics analysis.

Before analysis of the p53 mutant UV response we first needed to understand the wild-type UV response. It turned out that this response is highly biphasic, which was in a varying degree also found by others [48;49]. Many genes (1,427) change in the first three hours, hardly any (289) between 3 and 12 hours, and again many (1,756) from 12 to 24 hours. In total 2,856 genes were involved, which showed a remarkable specificity (80%) for being used in only one specific phase. The defined UV responsive categories with uniquely used genes were: Early (35%), Middle (4%), Late (47%), and the biphasic category: Early-Late (14%). Most of the Early responsive genes were repressed, which is in line with other studies [41;44;47]. Many Early-Late responsive genes showed an opposite gene-expression response in the Early versus Late phase.

In line, these genes lead to the identification of many cellular processes (i.e., GO-terms): 20 in Early, 3 in Middle, 34 in Late and 9 in Early-Late, which reflects the number of genes in each category. This clear biphasic UV response showed as Early processes; transcription, apoptosis, cell growth and cell cycle. The Late processes were: replication, cell proliferation, transport, adhesion and several metabolism processes. These Early and Late UV responses were reported earlier [42;44;45;47]. One study with an extensive time course, i.e., 0.5, 3, 6, 12 and 24 hours after UV exposure, also defined (five) different response phases. Although this was a UV-B response in human keratinocytes, many of the processes involved were comparable with our findings in the UV-C response in wild-type MEFs. So, the specificity of the UV light exposure, as well as cell type has little influence on the cellular response. It seems the early stress response after UV exposure results in direct activation of processes to avoid sustained DNA damages in cells like apoptosis, regulation of transcription to regulate all DNA damage response genes, and cell-cycle related processes. The Late responses are more related to re-entering the cell cycle again like DNA replication, nucleic acid metabolism and ATP synthesis. In the Early-Late responsive group the GO-term DNA repair, initiated by exposure to UV [19], was present. This DNA repair response might aim in the Early response at the immediate removal of DNA damage from actively transcribed DNA which is essential for the cell to survive, whereas in the Late response it might be directed to eliminate DNA damage from the overall genome. Another interesting finding is that several ubiquitin-related processes, required for marking

(old, damaged or misfolded) proteins for destruction, were found in Early, Late and Early-Late responses, indicating that this process plays a prominent role throughout the entire UV response.

III) Effect of p53.S389 phosphorylation on UV-induced gene expression in the specific phases

Whereas the ANOVA analysis revealed many genes for the term ‘Genotype’ and even more for the term ‘Time’, the interaction term ‘Genotype x Time’ showed no genes. This means that the ANOVA method is not powerful enough to identify the subtle changes in gene-expression, which is a common characteristic of ANOVA interaction terms. Aligning the analysis of the UV-responses in wild-type (6,058 genes) and p53.S389A (4,166 genes) MEFs resulted, as expected, in a major (3,558 genes) overlap (59% and 85%, respectively). However, also a considerable number of genes (3,108) were either not-found (80%) or newly-found (20%) to be significantly changed after UV exposure in p53.S389A compared to wild-type MEFs. This was expected, since phosphorylation of p53.S389 has been predominantly observed after UV exposure [12]. Of all genes involved in UV response, 14% showed an adjusted basal gene-expression level before exposure to UV radiation. Together, these findings point towards a system where a significant part of the p53-dependent gene-network is re-adjusted in response to the p53.S389A mutation, so that the response to UV exposure only results in minor differential expression responses of the involved p53-dependent genes and a weak differential phenotype response.

Extensive analysis of the affected biphasic UV response p53.S389A MEFs showed that phase I, early after UV exposure, appears mostly affected by the absence of Ser389 phosphorylation, with the absence of some processes dealing with cell cycle and apoptotic responses. It is tempting to speculate that when optimal transcriptional activation of genes and consequently functioning of proteins in these processes are adversely affected in cells, one can envision these cells will sustain more persistent DNA damages, and these damages might be fixed into gene mutations or other genetic alterations. This could be supported by the finding that the GO-term ‘cell division’ was gained in p53.S389A MEFs and increased levels of cell division are known to result in an increase in mutational load [50]. As a defense mechanism, the cell could increase levels or activity of processes like DNA repair or responses to DNA damage stimuli, however, these processes were shifted from phase I to phase III, pointing towards a delayed defense response in p53.S389A MEFs. Interestingly, the process ‘induction of apoptosis’, which was absent in phase I in p53.S389A MEFs, contained the UV-related apoptotic p53 target gene in MEFs; *Siva* [51]. P53.S389 phosphorylation is needed for an optimal response of this apoptotic target gene. Also, the GO-term ‘protein ubiquitination’, which was absent in phase I in UV-exposed p53.S389A MEFs, contains six relevant genes amongst which: *Fbxw*, the ubiquitin ligase implicated in the control of chromosome stability and furthermore identified as a p53-dependent tumor suppressor gene [52]; *Kcmf1*, identified as a potential metastasis suppressor [53]; p53-target gene *Mdm2*, functioning as a primary regulator of p53 [54]; *Vhhl*, playing a role in tumor suppression by participating as a component of p53 trans-activation complex during DNA damage response [55]; and *Wwp1*, recently identified as a Mdm2-independent regulator of p53 activity, which analogous to Mdm2 also showed a possible feedback loop mechanism [56]. All these genes display a role in DNA damage response pathways or are related to tumorigenic processes, all but one (*Kcmf1*) are clearly related to p53, and p53.S389 phosphorylation plays a role in their functioning.

Comparing this study with the p53.S389A bladders exposed to 2-AAF [14] we noticed distinct differences and similarities. In both studies there are genes observed with adjusted gene-expression level before exposure to the DNA damaging agent, though in MEFs many more than in bladder cells. This might relate to the *in-vitro* versus *in-vivo* set-up, as we experienced this difference in other studies as well. However, both studies showed corresponding affected processes, such as the p53-related pathways cell cycle arrest and apoptosis. However, in the 2-AAF-exposed p53.S389A bladders we found delayed gene-expression profiles, whereas in the UV-exposed p53.S389A MEFs an overall reduced expression profile was found. Of course the important differences in set-up will account at least partly for this: *in-vivo* versus *in-vitro*, different compounds (2-AAF versus UV), and different time-scale (weeks versus hours).

Finally, it is obvious that the analysis presented here, though already extensive, is just a starting point for such a complex transcriptomics experiment as described here. We have identified many processes involved in several p53 genotypes before and after UV exposure, each of which deserve to be further micro-dissected as to precisely determine what its role is in (p53-dependent) DNA-damaging responses and how it is affected by the absence of p53.S389 phosphorylation. As a preview on the complexity, we showed in Figure 5F the many (different) genes that are affected in some key processes in UV response, like 'DNA repair' and 'response to DNA damaging stimulus'. To comprehend the overall interactions, we need a broad model of the p53 network. As such, the updated model from Harris and Levine [30] (Figure 6) is a perfect starting point for this. We could already map our here described initial findings, which immediately will show the significance of p53.S389 phosphorylation in the major p53-induced pathways. Evidently, analysis of differential gene expression between wild-type and p53^{-/-} MEFs in this study has also exposed various new p53-dependent target genes (W. Bruins *et al.*, *manuscript in preparation*), and future studies will be aimed at demonstrating the p53 dependence of transcriptional activation of these genes and unraveling the pathways they are involved in.

In summary, we identified absence of a number of processes needed to negatively regulate tumor promoting processes, and furthermore gain of a number of processes positively regulating tumorigenic processes in our p53.S389A mutant MEFs after exposure to UV compared to wild-type MEFs. As a consequence, absence or decreased efficiency of p53.S389 phosphorylation may result in more initiated cells followed by increased incidences of (skin)tumors after exposure to UV, a phenomenon indeed observed when mice lacking this phosphorylation event are chronically exposed to UV [12]. Whether affected p53.S389 phosphorylation is also observed in humans (i.e., human p53.S392) and as such accounts for increased sensitivity for sun-light induced skin cancers, is an interesting question that needs to be addressed in follow-up studies.

Acknowledgements

We are grateful to M.M. Schaap for her assistance with the RT-PCR analyses, and Dr. R. Stad and Drs. H. Rauwerda for fruitful discussions. This work was supported by the Dutch Cancer Society (KWF) grant 2000-2352, NIH/NIEHS (Comparative Mouse Genomics Centers Consortium) grant 1U01 ES11044-02, and BSIK grant through the Netherlands Genomics Initiative (NGI) in the context of the BioRange program of the Netherlands Bioinformatics Centre (NBIC).

References

1. Ashcroft, M. and Vousden, K.H. (1999) Regulation of p53 stability. *Oncogene*, **18**, 7637-7643.
2. Lu, X. (2005) p53: a heavily dictated dictator of life and death. *Curr. Opin. Genet. Dev.*, **15**, 27-33.
3. Latonen, L., Taya, Y., and Laiho, M. (2001) UV-radiation induces dose-dependent regulation of p53 response and modulates p53-HDM2 interaction in human fibroblasts. *Oncogene*, **20**, 6784-6793.
4. Brooks, C.L. and Gu, W. (2006) p53 ubiquitination: Mdm2 and beyond. *Mol. Cell*, **21**, 307-315.
5. Appella, E. and Anderson, C.W. (2000) Signaling to p53: breaking the posttranslational modification code. *Pathol. Biol. (Paris)*, **48**, 227-245.
6. Lakin, N.D. and Jackson, S.P. (1999) Regulation of p53 in response to DNA damage. *Oncogene*, **18**, 7644-7655.
7. Bode, A.M. and Dong, Z. (2004) Post-translational modification of p53 in tumorigenesis. *Nat. Rev. Cancer*, **4**, 793-805.
8. Liu, G. and Chen, X. (2006) Regulation of the p53 transcriptional activity. *J. Cell Biochem.*, **97**, 448-458.
9. Kapoor, M. and Lozano, G. (1998) Functional activation of p53 via phosphorylation following DNA damage by UV but not gamma radiation. *Proc. Natl. Acad. Sci. U.S.A.*, **95**, 2834-2837.
10. Lu, H., Taya, Y., Ikeda, M., and Levine, A.J. (1998) Ultraviolet radiation, but not gamma radiation or etoposide-induced DNA damage, results in the phosphorylation of the murine p53 protein at serine-389. *Proc. Natl. Acad. Sci. U.S.A.*, **95**, 6399-6402.
11. Iwakuma, T. and Lozano, G. (2007) Crippling p53 activities via knock-in mutations in mouse models. *Oncogene*, **26**, 2177-2184.
12. Bruins, W., Zwart, E., Attardi, L.D., Iwakuma, T., Hoogervorst, E.M., Beems, R.B., Miranda, B., van Oostrom, C.T., van den, B.J., van den Aardweg, G.J., Lozano, G., van Steeg, H., Jacks, T., and de Vries, A. (2004) Increased sensitivity to UV radiation in mice with a p53 point mutation at Ser389. *Mol. Cell Biol.*, **24**, 8884-8894.
13. Hoogervorst, E.M., Bruins, W., Zwart, E., van Oostrom, C.T., van den Aardweg, G.J., Beems, R.B., van den, B. J., Jacks, T., van Steeg, H., and de Vries, A. (2005) Lack of p53 Ser389 phosphorylation predisposes mice to develop 2-acetylaminofluorene-induced bladder tumors but not ionizing radiation-induced lymphomas. *Cancer Res.*, **65**, 3610-3616.
14. Bruins, W., Jonker, M.J., Bruning, O., Pennings, J.L., Schaap, M.M., Hoogervorst, E.M., van, S.H., Breit, T.M., and de, V.A. (2007) Delayed Expression of Apoptotic and Cell Cycle Control Genes in Carcinogen-Exposed Bladders of Mice Lacking p53.S389 Phosphorylation. *Carcinogenesis*.
15. Mitchell, D.L., Haipek, C.A., and Clarkson, J.M. (1985) (6-4)Photoproducts are removed from the DNA of UV-irradiated mammalian cells more efficiently than cyclobutane pyrimidine dimers. *Mutat. Res.*, **143**, 109-112.
16. van Zeeland, A.A., Vreeswijk, M.P., de Gruijl, F.R., van Kranen, H.J., Vrieling, H., and Mullenders, L.F. (2005) Transcription-coupled repair: impact on UV-induced mutagenesis in cultured rodent cells and mouse skin tumors. *Mutat. Res.*, **577**, 170-178.
17. Latonen, L. and Laiho, M. (2005) Cellular UV damage responses-Functions of tumor suppressor p53. *Biochim. Biophys. Acta*, **1755**, 71-89.
18. Sachsenmaier, C., Radler-Pohl, A., Zinck, R., Nordheim, A., Herrlich, P., and Rahmsdorf, H.J. (1994) Involvement of growth factor receptors in the mammalian UVC response. *Cell*, **78**, 963-972.
19. Guo, Y.L., Chang, H.C., Tsai, J.H., Huang, J.C., Li, C., Young, K.C., Wu, L.W., Lai, M.D., Liu, H.S., and Huang, W. (2002) Two UVC-induced stress response pathways in HeLa cells identified by cDNA microarray. *Environ. Mol. Mutagen.*, **40**, 122-128.
20. Levine, A.J. (1997) p53, the cellular gatekeeper for growth and division. *Cell*, **88**, 323-331.
21. Corbet, S.W., Clarke, A.R., Gledhill, S., and Wylie, A.H. (1999) P53-dependent and -independent links between DNA-damage, apoptosis and mutation frequency in ES cells. *Oncogene*, **18**, 1537-1544.
22. Ko, L.J. and Prives, C. (1996) p53: puzzle and paradigm. *Genes Dev.*, **10**, 1054-1072.
23. Xu, D., Wilson, T.J., Chan, D., De Luca, E., Zhou, J., Hertzog, P.J., and Kola, I. (2002) Ets1 is required for p53 transcriptional activity in UV-induced apoptosis in embryonic stem cells. *EMBO J.*, **21**, 4081-4093.
24. Wang, Y. and Li, G. (2006) ING3 Promotes UV-induced Apoptosis via Fas/Caspase-8 Pathway in Melanoma Cells. *J. Biol. Chem.*, **281**, 11887-11893.
25. Brugarolas, J., Chandrasekaran, C., Gordon, J.I., Beach, D., Jacks, T., and Hannon, G.J. (1995) Radiation-induced cell cycle arrest compromised by p21 deficiency. *Nature*, **377**, 552-557.
26. Mootha, V.K., Lindgren, C.M., Eriksson, K.F., Subramanian, A., Sihag, S., Lehar, J., Puigserver, P., Carlsson, E.,

- Ridderstrale,M., Laurila,E., Houstis,N., Daly,M.J., Patterson,N., Mesirov,J.P., Golub,T.R., Tamayo,P., Spiegelman,B., Lander,E.S., Hirschhorn,J.N., Altshuler,D., and Groop,L.C. (2003) PGC-1alpha-responsive genes involved in oxidative phosphorylation are coordinately downregulated in human diabetes. *Nat. Genet.*, **34**, 267-273.
27. Polakis,P. (2007) The many ways of Wnt in cancer. *Curr. Opin. Genet. Dev.*, **17**, 45-51.
 28. Draghici,S., Khatri,P., Bhavsar,P., Shah,A., Krawetz,S.A., and Tainsky,M.A. (2003) Onto-Tools, the toolkit of the modern biologist: Onto-Express, Onto-Compare, Onto-Design and Onto-Translate. *Nucleic Acids Res.*, **31**, 3775-3781.
 29. van Delft,J.H., van Agen,E., van Breda,S.G., Herwijnen,M.H., Staal,Y.C., and Kleinjans,J.C. (2004) Discrimination of genotoxic from non-genotoxic carcinogens by gene expression profiling. *Carcinogenesis*, **25**, 1265-1276.
 30. Harris,S.L. and Levine,A.J. (2005) The p53 pathway: positive and negative feedback loops. *Oncogene*, **24**, 2899-2908.
 31. Appella,E. and Anderson,C.W. (2001) Post-translational modifications and activation of p53 by genotoxic stresses. *Eur.J.Biochem.*, **268**, 2764-2772.
 32. Thompson,T., Tovar,C., Yang,H., Carvajal,D., Vu,B.T., Xu,Q., Wahl,G.M., Heimbrook,D.C., and Vassilev,L.T. (2004) Phosphorylation of p53 on key serines is dispensable for transcriptional activation and apoptosis. *J.Biol.Chem.*, **279**, 53015-53022.
 33. Jackson,M.W., Agarwal,M.K., Agarwal,M.L., Agarwal,A., Stanhope-Baker,P., Williams,B.R., and Stark,G.R. (2004) Limited role of N-terminal phosphoserine residues in the activation of transcription by p53. *Oncogene*, **23**, 4477-4487.
 34. Zschenker,O., Borgmann,K., Streichert,T., Meier,I., Wrona,A., and Dikomey,E. (2006) Lymphoblastoid cell lines differing in p53 status show clear differences in basal gene expression with minor changes after irradiation. *Radiother.Oncol.*, **80**, 236-249.
 35. Coates,P.J., Lorimore,S.A., and Wright,E.G. (2005) Cell and tissue responses to genotoxic stress. *J.Pathol.*, **205**, 221-235.
 36. Xie,S., Wang,Q., Wu,H., Cogswell,J., Lu,L., Jhanwar-Uniyal,M., and Dai,W. (2001) Reactive oxygen species-induced phosphorylation of p53 on serine 20 is mediated in part by polo-like kinase-3. *J.Biol.Chem.*, **276**, 36194-36199.
 37. Macip,S., Igarashi,M., Berggren,P., Yu,J., Lee,S.W., and Aaronson,S.A. (2003) Influence of induced reactive oxygen species in p53-mediated cell fate decisions. *Mol.Cell Biol.*, **23**, 8576-8585.
 38. Huang,M., Wang,Y., Sun,D., Zhu,H., Yin,Y., Zhang,W., Yang,S., Quan,L., Bai,J., Wang,S., Chen,Q., Li,S., and Xu,N. (2006) Identification of genes regulated by Wnt/beta-catenin pathway and involved in apoptosis via microarray analysis. *BMC.Cancer*, **6**, 221.
 39. Harvey,M., Sands,A.T., Weiss,R.S., Hegi,M.E., Wiseman,R.W., Pantazis,P., Giovannella,B.C., Tainsky,M.A., Bradley,A., and Donehower,L.A. (1993) In vitro growth characteristics of embryo fibroblasts isolated from p53-deficient mice. *Oncogene*, **8**, 2457-2467.
 40. Boerma,M., van der Wees,C.G., Vrieling,H., Svensson,J.P., Wondergem,J., van der,L.A., Mullenders,L.H., and van Zeeland,A.A. (2005) Microarray analysis of gene expression profiles of cardiac myocytes and fibroblasts after mechanical stress, ionising or ultraviolet radiation. *BMC.Genomics*, **6**, 6.
 41. Gentile,M., Latonen,L., and Laiho,M. (2003) Cell cycle arrest and apoptosis provoked by UV radiation-induced DNA damage are transcriptionally highly divergent responses. *Nucleic Acids Res.*, **31**, 4779-4790.
 42. Zhao,R., Gish,K., Murphy,M., Yin,Y., Notterman,D., Hoffman,W.H., Tom,E., Mack,D.H., and Levine,A.J. (2000) Analysis of p53-regulated gene expression patterns using oligonucleotide arrays. *Genes Dev.*, **14**, 981-993.
 43. Yang,G., Zhang,G., Pittelkow,M.R., Ramoni,M., and Tsao,H. (2006) Expression Profiling of UVB Response in Melanocytes Identifies a Set of p53-Target Genes. *J.Invest Dermatol.*, **126**, 2490-2506.
 44. Sesto,A., Navarro,M., Burslem,F., and Jorcano,J.L. (2002) Analysis of the ultraviolet B response in primary human keratinocytes using oligonucleotide microarrays. *Proc.Natl.Acad.Sci.U.S.A.*, **99**, 2965-2970.
 45. Enk,C.D., Jacob-Hirsch,J., Gal,H., Verbovetski,I., Amariglio,N., Mevorach,D., Ingber,A., Givol,D., Rechavi,G., and Hochberg,M. (2006) The UVB-induced gene expression profile of human epidermis in vivo is different from that of cultured keratinocytes. *Oncogene*.
 46. Amundson,S.A., Do,K.T., Vinikoor,L., Koch-Paiz,C.A., Bittner,M.L., Trent,J.M., Meltzer,P., and Fornace,A.J., Jr. (2005) Stress-specific signatures: expression profiling of p53 wild-type and -null human cells. *Oncogene*, **24**, 4572-4579.

47. Dazard,J.E., Gal,H., Amariglio,N., Rechavi,G., Domany,E., and Givol,D. (2003) Genome-wide comparison of human keratinocyte and squamous cell carcinoma responses to UVB irradiation: implications for skin and epithelial cancer. *Oncogene*, **22**, 2993-3006.
48. Kannan,K., Kaminski,N., Rechavi,G., Jakob-Hirsch,J., Amariglio,N., and Givol,D. (2001) DNA microarray analysis of genes involved in p53 mediated apoptosis: activation of Apaf-1. *Oncogene*, **20**, 3449-3455.
49. Kannan,K., Amariglio,N., Rechavi,G., Jakob-Hirsch,J., Kela,I., Kaminski,N., Getz,G., Domany,E., and Givol,D. (2001) DNA microarrays identification of primary and secondary target genes regulated by p53. *Oncogene*, **20**, 2225-2234.
50. Hoogervorst,E.M., van Oostrom,C.T., Beems,R.B., van Benthem,J., Gielis,S., Vermeulen,J.P., Wester,P. W., Vos,J.G., de Vries,A., and van Steeg,H. (2004) p53 heterozygosity results in an increased 2-acetylaminofluorene-induced urinary bladder but not liver tumor response in DNA repair-deficient Xpa mice. *Cancer Res.*, **64**, 5118-5126.
51. Jacobs,S.B., Basak,S., Murray,J.I., Pathak,N., and Attardi,L.D. (2007) Siva is an apoptosis-selective p53 target gene important for neuronal cell death. *Cell Death.Differ.*.
52. Mao,J.H., Perez-Losada,J., Wu,D., Delrosario,R., Tsunematsu,R., Nakayama,K.I., Brown,K., Bryson,S., and Balmain,A. (2004) Fbxw7/Cdc4 is a p53-dependent, haploinsufficient tumour suppressor gene. *Nature*, **432**, 775-779.
53. Kreppel,M., Aryee,D.N., Schaefer,K.L., Amann,G., Kofler,R., Poremba,C., and Kovar,H. (2006) Suppression of KCMF1 by constitutive high CD99 expression is involved in the migratory ability of Ewing's sarcoma cells. *Oncogene*, **25**, 2795-2800.
54. Kubbutat,M.H., Jones,S.N., and Vousden,K.H. (1997) Regulation of p53 stability by Mdm2. *Nature*, **387**, 299-303.
55. Roe,J.S. and Youn,H.D. (2006) The positive regulation of p53 by the tumor suppressor VHL. *Cell Cycle*, **5**, 2054-2056.
56. Laine,A. and Ronai,Z. (2007) Regulation of p53 localization and transcription by the HECT domain E3 ligase WWP1. *Oncogene*, **26**, 1477-1483.

Supplementary Tables

<http://www.microarray.nl/mef-uv.html>